

Studies of Surface Coverage and Orientation of DNA Molecules Immobilized onto Preformed Alkanethiol Self-Assembled Monolayers

Eva Huang, Feimeng Zhou,* and Le Deng

Department of Chemistry and Biochemistry, California State University, Los Angeles,
Los Angeles, California 90032

Received August 10, 1999. In Final Form: December 13, 1999

DNA molecules are attached onto carboxylate-terminated alkanethiol self-assembled monolayers (SAMs) preformed at gold surfaces via the *N*-hydroxysulfosuccinimide (NHS)/1-(3-(dimethylamino)propyl)-3-ethylcarbodiimide hydrochloride (EDC) cross-linking reaction. Cyclic voltammetry, quartz crystal microbalance (QCM), and atomic force microscopy (AFM) were used to probe the surface coverage and molecular orientation of the immobilized DNA molecules. The DNA attachment is attributed to the formation of amide bond between the carboxylate groups and the amino groups on the DNA bases since the possibility of nonspecific adsorption of DNA onto preformed SAMs or NHS ester monolayers was studied and excluded. Our voltammetric results indicate a significant blockage of the sites originally available in the alkanethiol SAMs for facile heterogeneous electron transfer by the attached DNA molecules. QCM provided a semiquantitative measurement of the amount of immobilized DNA. The AFM images, for the first time, revealed that relatively ordered DNA films can be formed in the covalent attachment with DNA molecules stretched by the underlying terminal carboxylate groups of the SAMs. However, certain fragmentation appears to have occurred upon immobilization. The fragmentation is probably due to the strong interaction between the DNA molecules and the carboxylate groups whose spatial distribution does not fit perfectly well with the separation and distribution of the amino groups on the bases within the DNA double helix.

1. Introduction

Sensitive and selective detection of a target DNA of a specific sequence by a DNA probe immobilized onto a solid surface (i.e., heterogeneous DNA sensors) is a powerful analytical technique in modern molecular biology.^{1–5} Among the various types of sensing devices developed, electrochemically based DNA biosensors have received a great deal of attention^{6–16} owing to the high sensitivity and rapid speed of electrochemical detection and the low cost of the electrochemical instrumentation.¹⁷

Despite the tremendous potential of a miniaturized heterogeneous electrochemical DNA biosensor, there is a general lack of fundamental knowledge about the steps involved in the fabrication of and sensing by a DNA-modified electrode/metal surface. For example, the solution and surface conditions affecting DNA adsorption, the optimal time for DNA immobilization, and the surface coverage and orientation of immobilized DNA are important parameters.^{1–5} However, these parameters were generally not well understood and little effort had been made to relate them to the ultimate analytical performance of the heterogeneous DNA sensor. Recently, more sensor developers are beginning to pay attention to the understanding at the molecular level about the relationship between the properties of the DNA-modified surfaces and the analytical “figures of merit” of potentially useful sensors. Using thiol-tethered oligonucleotides mixed with alkanethiol self-assembled monolayers (SAMs) formed at gold surfaces, Tarlov and co-workers carried out a systematic investigation on the effect of molecular orientations at probe surfaces on their efficiency in hybridizing the target molecules.^{18–21} The dependence of DNA molecular orientation on the applied potential and electron-transfer reactions at similar DNA SAM-modified electrodes were studied by Barton and co-workers.^{22,23} A theoretical model that treats the DNA hybridization as a

- (1) Wetmur, J. G. *Crit. Rev. Biochem. Mol. Biol.* **1991**, *26*, 227–259.
- (2) Watson, J.; Gilman, M.; Witkowski, J.; Zoller, M. *Recombinant DNA*, 2nd ed.; W. H. Freeman and Co.: New York, 1992.
- (3) Anderson, M. L. M. *Nucleic Acid Hybridization*, 1st ed.; Springer-Verlag: New York, 1998.
- (4) Chan, V.; Graves, D. J.; McKenzie, S. E. *Biophys. J.* **1995**, *69*, 2243–2255.
- (5) Englisch, U.; Gauss, D. H. *Angew. Chem., Int. Ed. Engl.* **1991**, *30*, 613–722.
- (6) Bard, A. J.; Carter, M. T.; Rodriguez, M. J. *Am. Chem. Soc.* **1989**, *111*, 8901–8911.
- (7) Bard, A. J.; Xu, X.-H. *J. Am. Chem. Soc.* **1995**, *117*, 2627–2631.
- (8) Mikkelsen, S. R.; Millan, K. M. *Anal. Chem.* **1993**, *65*, 2317–2323.
- (9) Mikkelsen, S. R.; Millan, K. M.; Sarullo, A. *Anal. Chem.* **1994**, *66*, 2943–2948.
- (10) Wang, J.; Cai, X.; Rivas, G.; Farias, P. *Anal. Chem.* **1996**, *68*, 2629–2633.
- (11) Wang, J.; Palecek, E.; Nielsen, P.; Rivas, G.; Cai, X.; Shiraishi, H.; Dontha, N.; Luo, D.; Farias, P. *J. Am. Chem. Soc.* **1996**, *118*, 7667–7670.
- (12) Pandey, P. C.; Weetall, H. H. *Anal. Chem.* **1994**, *66*, 1236–1241.
- (13) Carvana, D. J.; Heller, A. *J. Am. Chem. Soc.* **1999**, *121*, 769–774.
- (14) Hashimoto, K.; Ito, K.; Ishimori, Y. *Anal. Chim. Acta* **1994**, *286*, 219–224.
- (15) Whittemore, N. A.; Mullenix, A. N.; Inamati, G. B.; Manoharan, M.; Cook, P. D.; Tuinman, A. A.; Baker, D. C.; Chambers, J. Q. *Bioconjugate Chem.* **1999**, *10*, 261–270.
- (16) Zhao, Y.-D.; Pang, D.-W.; Wang, Z.-L.; Cheng, J.-K. *J. Electroanal. Chem.* **1997**, *431*, 203–209.
- (17) Bard, A. J.; Faulkner, L. R. *Electrochemical Methods. Fundamentals and Applications*; John Wiley & Sons: New York, 1980.

- (18) Peterlinz, K. A.; Georgiadis, R. M.; Herne, T. M.; Tarlov, M. J. *J. Am. Chem. Soc.* **1997**, *119*, 3401–3402.
- (19) Steel, A. B.; Herne, T. M.; Tarlov, M. J. *Anal. Chem.* **1998**, *70*, 4670–4677.
- (20) Herne, T. M.; Tarlov, M. J. *J. Am. Chem. Soc.* **1997**, *119*, 8916–8920.
- (21) Levicky, R.; Herne, T. M.; Tarlov, M. J.; Satija, S. K. *J. Am. Chem. Soc.* **1998**, *120*, 9787–9792.
- (22) Kelley, S. O.; Barton, J. K.; Jackson, N. M.; McPherson, L. D.; Porter, A. B.; Spain, E. M.; Allen, M. J.; Hill, M. G. *Langmuir* **1998**, *14*, 6781–6784.
- (23) Barton, J. K.; Hill, M. G.; Kelley, S. O.; Jackson, N. M. *Bioconjugate Chem.* **1997**, *8*, 31–37.

combined irreversible reaction–diffusion process was reported in an attempt to predict important factors for an efficient hybridization reaction.⁴ These studies demonstrated that, for the development of a new sensor or the improvement of an existing sensor, a good understanding of the structure–function relationship of the immobilized DNA molecules is necessary.

While the thiol-modified DNA films probably provide a very well organized system for surface characterization, the methodology is mainly suitable to the anchoring of chemically modified oligonucleotides. For the immobilization of relatively large and/or unmodified DNA molecules, other means based on different surface chemical reactions are more appropriate. Owing to such a necessity, a number of schemes have been explored for immobilizing single- and double-stranded DNA molecules. Some of the schemes include, but are not limited to, the use of carbodiimide-activated carboxylic acid impregnated into carbon paste⁹ or produced from oxidizing carbon surface⁸ to form amide bonds with the DNA bases, the attachment of avidin onto dithiodipropionic acid for subsequent attachment of biotinylated DNA,²⁴ the formation of positively charged aluminum alkanebisphosphate thin film for electrostatically accumulating DNA,²⁵ and, more recently, the immobilization of DNA with a tethered intercalator affixed to the solution end of a SAM film.²⁶ We decided to carry out surface characterization and quantification of polynucleotides anchored onto preformed alkanethiol SAMs via the cross-linking reaction using *N*-hydroxysulfosuccinimide (NHS) and 1-(3-(dimethylamino)propyl)-3-ethylcarbodiimide hydrochloride (EDC).^{27–29} The choice of this system is based on the following three considerations: First, immobilization of proteins and nucleic acids based on the NHS/EDC cross-linking methodology is one of the most popular means for construction of biosensors.^{8,9,30–35} However, to date, few reports^{8,9,24} that were concerned with the use of carbodiimide-activated carboxylic acids to anchor nucleic acids have characterized the electrode surfaces or attempted to quantify the amount of immobilized DNA molecules. Rather, the published procedures rely on either an indirect monitoring of the hybridization reaction²⁴ or on an indicator compound incorporated into double-stranded DNA molecules for the feasibility studies of the immobilization method.^{8,9} Furthermore, some of the surfaces/systems employed are difficult to characterize and could introduce ambiguity. For example, Mikkelsen et al. showed that polynucleotides can be attached to the carboxylic acid present at oxidized glassy carbon surfaces⁸ or to aliphatic carboxylic acids (e.g., stearic acid⁹) mixed into a carbon paste electrode. While such an approach affords simple electrochemically based DNA sensors, the rough and complex carbon paste

or glassy carbon surfaces are not suitable for certain surface characterization techniques³⁶ (e.g., atomic force microscopy used in this study). Furthermore, given the complexity and activity of carbon surface,³⁷ it is not clear if some of the surface-confined DNA molecules were due to nonspecific adsorption. In addition, the random distribution of the carboxylate groups could introduce uncertainty to the quantification of the amount of immobilized DNA per unit area and to the estimate of the surface coverage of DNA (e.g., atomic force microscopy (AFM) and quartz crystal microbalance³⁸ employed in the present work). Our second consideration in choosing the current system is, therefore, to circumvent these problems by using alkanethiol SAMs formed onto gold surfaces. Alkanethiol SAMs are known to produce well-ordered structures that can be tailored by changing the conditions for adsorption and by varying the functional groups on the alkyl chains. Owing to these unique features, Corn and co-workers successfully attached poly(L-lysine) monolayers onto preformed alkanethiol monolayers through amide bond formation.^{30,31} Other protein molecules, such as clathrin,³³ catalase,³² and cytochromes^{39,40} have also been covalently attached to the solution termini of the alkanethiol SAMs via covalent bonding or electrostatic interactions. The third reason we chose this system is that gold surfaces and alkanethiol SAM-modified gold surfaces are model systems that are amenable to surface characterization techniques such as AFM,⁴¹ scanning tunneling microscopy (STM),⁴² and surface plasmon resonance.⁴³ For instance, Patel et al. recently reported STM and tapping mode AFM images of catalase adsorbed onto two different alkanethiol SAMs.³² The tremendous amount of previous work on the characterization of alkanethiol SAMs^{42,44–47} with scanning probe microscopy enables one to control the film formation and the subsequent DNA attachment while reducing the ambiguity in data interpretation. Most importantly, magnetic alternating current mode AFM has become a powerful and indispensable technique for studying immobilized DNA molecules and DNA-involving surface processes.^{48–51} Therefore, by choosing an immobilization scheme whose chemistry has been thoroughly studied and utilizing surfaces that are amenable to surface characterization techniques, it is expected that fundamental knowledge about the resultant DNA films can be acquired. In this

(24) Caruso, F.; Rodda, E.; Furlong, D. F.; Niikura, K.; Okahata, Y. *Anal. Chem.* **1997**, *69*, 2043–2049.

(25) Carter, M. T.; Rodriguez, M.; Bard, A. J. *J. Am. Chem. Soc.* **1989**, *111*, 8901–8911.

(26) Higashi, N.; Takahashi, M.; Niwa, M. *Langmuir* **1999**, *15*, 111–115.

(27) Swingle, D. M.; Staros, J. V.; Wright, R. W. *Anal. Biochem.* **1986**, *156*, 220–222.

(28) Stefanowicz, P.; Siemion, I. Z. *Pol. J. Chem.* **1992**, *66*, 111–118.

(29) Mattson, G.; Conkin, E.; Desai, S.; Nielander, G.; Savage, M. D.; Morgensen, S. *Mol. Biol. Rep.* **1993**, *17*, 167–183.

(30) Corn, R. M.; Frey, B. L.; Jordan, C. E.; Kornguth, S. *Anal. Chem.* **1995**, *67*, 4452–4457.

(31) Corn, R. M.; Frey, B. L. *Anal. Chem.* **1996**, *68*, 3187–3193.

(32) Patel, N.; Davies, M. C.; Hartshorne, M.; Heaton, R. J.; Tendler, S. J. B.; Williams, P. M. *Langmuir* **1997**, *13*, 6485–6490.

(33) Wagner, P.; Kernen, P.; Hegner, M.; Ungewickell, E.; Semenza, G. *FEBS Lett.* **1994**, *356*, 267–271.

(34) Wagner, P.; Hegner, M.; Kernen, P.; Semenza, G. *J. Vac. Sci. Technol., B* **1996**, *14*, 1466–1471.

(35) Prime, K.; Whitesides, G. M. *Science* **1991**, *252*, 1164–1167.

(36) Magonov, S. N.; Whangbo, M.-H. *Surface Analysis with STM and AFM*; VCH Publishers and VCH Verlagsgesellschaft: New York and Weinheim, 1996.

(37) McCreery, R. L. In *Electroanalytical Chemistry*; Bard, A. J., Ed.; Marcel Dekker: New York, 1991; Vol. 17.

(38) Buttry, D. A. In *Electroanalytical Chemistry*; Bard, A. J., Ed.; Marcel Dekker: New York, 1991; Vol. 17.

(39) Glenn, J. D. H.; Bowden, E. F. *Chem. Lett.* **1996**, 399–400.

(40) El Kasmi, A.; Walden, J. M.; Bowden, S. B.; Linderman, R. J. *J. Am. Chem. Soc.* **1998**, *120*, 225–226.

(41) Noy, A.; Vezenov, D. V.; Lieber, C. M. *Annu. Rev. Mater. Sci.* **1997**, *37*, 381–421.

(42) Porter, M. D.; Widrig, C. A.; Alves, C. A. *J. Am. Chem. Soc.* **1991**, *113*, 2805–2810.

(43) Peterlinz, K. A.; Georgiadis, R. M. *Langmuir* **1996**, *12*, 4731–4740.

(44) McDermott, C. A.; McDermott, M. T.; Green, J.-B.; Porter, M. D. *J. Phys. Chem.* **1995**, *99*, 13257–13267.

(45) Wong, S.-S.; Takano, H.; Porter, M. D. *Anal. Chem.* **1998**, *70*, 5209–5212.

(46) Gerwith, A. A.; Niece, B. K. *Chem. Rev.* **1997**, *97*, 1129–1162.

(47) Schoer, J. K.; Crooks, R. M. *Langmuir* **1997**, *13*, 2322–2332.

(48) Hansma, H. G.; Hoh, J. H. *Annu. Rev. Biomol. Struct.* **1994**, *23*, 115–139.

(49) Bottomley, L. A. C.; Joseph, E.; Anderson, J. R.; McFail-Isom, L.; Williams, L. D. *J. Am. Chem. Soc.* **1997**, *119*, 3792–3796.

(50) Han, W.; Dlakic, M.; Zhu, J. Y.; Lindsay, S. M.; Harrington, R. E. *Proc. Natl. Acad. Sci. U.S.A.* **1997**, *94*, 10565–10575.

(51) Yang, X.; Wenzler, L. A.; Qi, J.; Li, X.; Seeman, N. C. *J. Am. Chem. Soc.* **1998**, *120*, 9779–9786.

work, our goals were to quantify the amount of immobilized double-stranded DNA molecules and to compare the orientation and/or surface coverage of the covalently attached DNA molecules to that of DNA electrostatically adsorbed onto solid surfaces. Findings from such studies should shed light on the important parameters related to the improvement of existing heterogeneous DNA biosensors and future design of potentially useful DNA sensing devices.

2. Experimental Section

Materials. Calf thymus DNA, double-stranded polydeoxyguanylic-polydeoxycytidylic acid (poly[dG]·poly[dC]), and benzylamine were purchased from Sigma (St. Louis, MO) and stored at -4°C . DNA solutions with an A_{260}/A_{280} ratio of 1.725 were prepared in a pH 7.0 phosphate buffer. No attempts were made to purify the DNA. *N*-Hydroxysulfosuccinimide (NHS) was obtained from Pierce (Rockford, IL) while triethanolamine hydrochloride (TEA), ω -mercaptoundecanoic acid (MUA), 1-(3-dimethylaminopropyl)-3-ethylcarbodiimide hydrochloride (EDC), 2,6-anthraquinonedisulfonic acid (AQS), and (3-aminopropyl)-triethoxysilane (APTES) were all acquired from Aldrich Chemicals (Milwaukee, WI). Hexaamineruthenium (III) chloride (RuHex, Strem Chemicals, Inc., Newburyport, MA) was used for the "blockage experiment" described below. A type GS filter (0.22 μm) was purchased from Millipore (Bedford, MA). All solutions were prepared with water treated with a Millipore water purification system.

Solution Preparation. TEA buffer used in this work contained 0.05 M TEA and 0.25 M NaCl (pH = 8.0). DNA solutions were prepared with a 0.1 M phosphate buffer stock solution whose pH was adjusted to 7.0 using a 0.1 M NaOH solution. NHS/EDC mixture solutions were produced by mixing 15 mM NHS and 75 mM EDC in phosphate buffer. The 1.0 mM MUA solution used was made by dissolving MUA in ethanol.

Instrumentation. The potentiostat for cyclic voltammetric experiments was a CH electrochemical analyzer (model 832, CH Instruments, Cordova, TN). The quantification of the amount of immobilized DNA was made possible using a home-built quartz crystal microbalance (QCM) that utilizes a Fluke PM 6680B frequency counter (Everett, WA) and an oscillator constructed based on the circuitry originally designed by Professor D. Buttry (University of Wyoming). Atomic force microscopic images were collected using an atomic force microscope (AFM) that is also equipped with a magnetic alternating current mode (MAC mode AFM, Molecular Imaging, Phoenix, AZ). The MAC cantilever tips (Molecular Imaging) used had a spring constant of 0.5 N/m.

Electrodes, Cells, and Substrates. Gold electrodes (3 mm diameter) were purchased from CH Instruments. Before use, they were first polished with diamond pastes down to 1 μm , followed by sonication in a water bath. The QCM crystals used for the quantification of immobilized DNA were 10 MHz crystals that were coated with polished gold disks (5 mm in diameter) on both sides (ICM Technologies, Oklahoma City, OK). Gold (111) substrates on mica used for AFM images either were purchased from Molecular Imaging or were generously provided by Dr. N. Tao (Florida International University). Mica substrates were obtained from Asheville Mica Co. (Newport News, VA).

Procedures. (a) Formation of MUA SAMs and Subsequent DNA Attachment. A typical procedure involves soaking gold electrodes, gold films, or the gold-coated QCM crystals for 1 h in 1 mM MUA ethanoic solution. On the basis of the voltammetric "blockage experiment" and AFM images described below, variation of the immersion time between 1 and 4 h did not appear to affect the organization of the MUA SAMs. Such an observation is in good agreement with the STM studies of *n*-octadecanethiolate monolayers performed by Porter et al.⁴² We also compared the effectiveness of DNA attachment at MUA films formed for 1 and 4 h and did not observe pronounced differences in terms of DNA surface coverage (see below in connection with the discussion of our voltammetric results). Therefore, we decided to use 1 h soaking time since the AFM gold substrates tend to peel off the mica surface upon extensive soaking. Upon immersion in MUA, the gold surfaces were then rinsed with absolute ethanol, followed by soaking in deionized

water for about 5 min. In the one-step reaction (see Figure 1 and the discussion of the reactions in the Results and Discussion section), the substrate surfaces were immersed in a solution containing 15 mM NHS, 75 mM EDC, and DNA of a chosen concentration (5–100 $\mu\text{g}/\text{mL}$) for approximately 4 h. The optimal DNA concentration for producing maximum DNA surface coverage was found to be above 10 $\mu\text{g}/\text{mL}$. Therefore we typically employed 25 or 50 $\mu\text{g}/\text{mL}$ DNA concentrations for our CV, QCM, and AFM work. Finally, the DNA-covered electrode or substrate was soaked in a 50 mM AQS/0.1 M phosphate buffer solution for overnight. During AQS intercalation into the DNA base stacks, the AQS solution was stirred to enhance the intercalation rate.

(b) Cyclic Voltammetry. Voltammetry of AQS at gold electrodes modified with DNA was compared to that at MUA-modified gold electrodes that had been subject to the NHS/EDC reaction and to gold electrodes modified with only MUA, respectively. To verify the adsorbate nature of the intercalator, scan rates ranging from 0.025 to 0.5 V/s were employed to study the scan-rate dependence of the peak current. To identify the presence of DNA, the extent of blockage of the heterogeneous electron transfer of RuHex in solution by the DNA-modified electrode was gauged. Its voltammetric behavior was then compared to that observed at a bare electrode, an electrode modified with MUA, and an MUA-covered electrode that was also reacted with the NHS/EDC mixture. All the electrodes used have identical geometrical area. To obtain supportive evidence about amide bond formation between DNA bases and activated carboxylic acid, the DNA immobilization was also carried out for 4 h at MUA-modified electrodes in the presence of benzylamine whose concentration (~ 4.58 mM) was 6 orders of magnitude greater than the DNA concentration (~ 4.67 nM). The electrodes were rinsed with deionized water and transferred into 50 μM AQS/phosphate buffer solutions which were stirred overnight. Upon overnight soaking, voltammograms were collected at these electrodes in AQS-free TEA buffer solutions under a nitrogen blanket.

(c) QCM. A typical QCM experiment begins with the cleaning of the crystal surface with a piranha solution (30% H_2O_2 and 70% concentrated H_2SO_4). *CAUTION: Piranha solution reacts violently with organic solvents and is a skin irritant. Extreme caution should be exercised when handling piranha solution.* After being rinsed with deionized water, the crystal was dried over a stream of N_2 gas. Sometimes an UV-Clean (model 135500, Boekel Industries Inc., Feasterville, PA) was used to scavenge hydrocarbon adsorbates. Next, the crystal was soaked in a 1 mM MUA solution for about 1 h. The crystal was then rinsed and mounted onto the QCM cell (ICM, Oklahoma City, OK) for the NHS/EDC reaction and/or the DNA attachment for 4 h. After reaction, the crystal was rinsed with deionized water and dried under a stream of N_2 and its frequency was measured. The magnitudes of frequency change caused by the attachment of only NHS and that attributable to the cumulative anchoring of both NHS and DNA molecules were then compared. The frequency difference can then be used to calculate the amount of immobilized DNA (see Results and Discussion).

(d) AFM. Vacuum-deposited gold (111) was first cleaned in the UV-Clean for 15 min followed by annealing in a hydrogen flame. The MUA formation and DNA attachment were carried out in the same manner as that for quartz crystals. The substrate covered with DNA was rinsed with deionized water three times before imaging in a phosphate buffer solution. The phosphate buffer solution was filtered with the 0.22 μm Millipore filter prior to use. AFM topographical, deflection, and phase images were obtained with an oscillating frequency of 25 kHz and a driver current of 30 ± 5 A. The amplitude change of the probe was low and therefore the imaging was essentially nondestructive to the sample.^{52,53}

3. Results and Discussion

DNA Immobilization Scheme. Figure 1 shows schematically the DNA immobilization scheme and the following intercalation step that is necessary for voltammetric

(52) Han, W.; Lindsay, S. M. *Appl. Phys. Lett.* **1998**, *72*, 1656–1658.

(53) Lindsay, S. M.; Han, W.; Jing, T.; Zhu, J.; Hudson, J. *J. Biol. Struct. Dyn.* **1998**, *16*, 151–155.

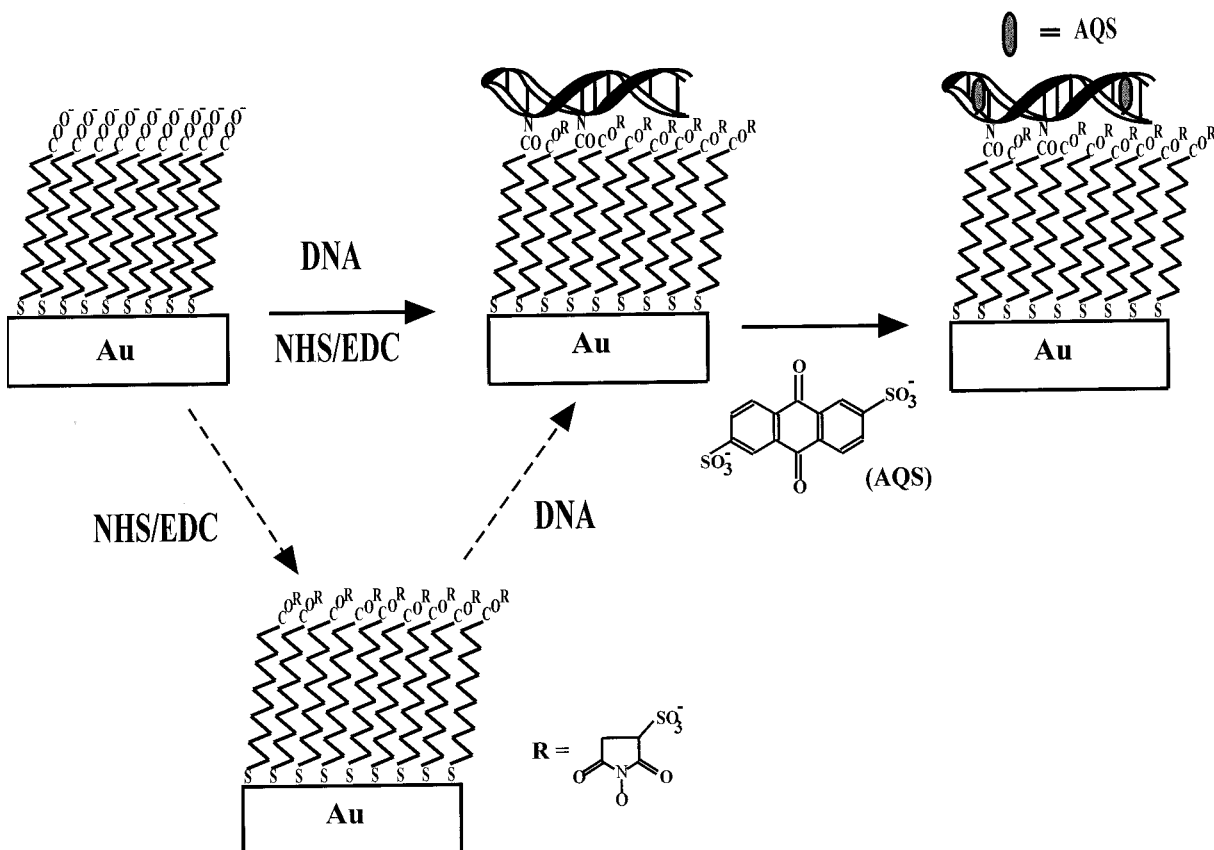


Figure 1. Schematic representation of the DNA immobilization scheme. The attachment of DNA molecules to the solution termini of the deprotonated MUA molecules can be accomplished via either the one-step reaction in a solution containing NHS, EDC, and DNA or the preformation of the NHS esters and the subsequent replacement of some ester groups by DNA in a separate solution (route indicated by the dotted arrows). EDC activates the carboxylic acid while NHS forms a stable ester with the activated carboxylate to impede hydrolysis of the activated carboxylic acid back to the original reactant. Verification of presence of DNA is achieved by voltammetric detection of 2,6-anthroquinonedisulfonic acid (AQS) that has been intercalated into the DNA double helices.

detection. This scheme is simplified from the procedures of Corn and Patel for protein attachment.^{30–32} MUA SAMs formed at gold substrates were exposed to a phosphate buffer solution containing NHS, EDC, and the DNA of interest. The pH of the phosphate buffer was 7.0, and therefore the MUA molecules were deprotonated.³¹ As commonly known,^{27–29} EDC will activate the carboxylate group at the MUA terminal, a step critical for the formation of an amide bond between the carboxylate groups and the primary amino groups on the DNA bases. The role of the NHS is to form the NHS ester intermediate (structure shown in the two-step procedure in Figure 1), preventing the *O*-acylurea formed during EDC activation of the carboxylate groups from hydrolyzing back to the original reactant.^{27–29} In our approach, unlike most researchers who conducted the NHS/EDC reaction and the DNA anchoring in two separate steps^{8,31,32} (the route indicated by the dotted arrows in Figure 1), we found that mixing NHS/EDC with DNA produced similar surfaces, based on the observations from our voltammetric and AFM experiments described later. It appears that there is no apparent advantage in producing the NHS ester intermediates then in a separate step forming the amide bond. In fact, Mattson et al. pointed out that the NHS/EDC cross-linking is more commonly carried out in the one-step manner.²⁹ It is worth mentioning that in our current work the unreacted NHS ester intermediates were not scavenged with any amines but left to be consumed in hydrolysis reactions. Therefore, the single-step reaction was more time effective than the common two-step immobilization scheme in which DNA

molecules replace the NHS esters following the NHS/EDC reaction performed in a separate solution.

As stated in the Experimental Section, a phosphate buffer was used to prepare the NHS, EDC, and DNA solutions. The use of a buffer solution was to overcome the electrostatic repulsion between the DNA polyanions and the negatively charged NHS esters originated from the sulfonate groups on the NHS esters. Such a step allows DNA molecules to approach to the vicinity of the NHS ester-containing SAMs so that the subsequent nucleophilic substitution of the NHS ester by the amino groups on DNA can take place.

In the final step, a suitable electroactive DNA intercalator (in this case, AQS) was incorporated into the DNA helices so that voltammetry becomes amenable to the detection and characterization of surface-immobilized DNA molecules.

Cyclic Voltammetry Characterization. Voltammetry is commonly utilized to estimate the surface coverage of adsorbates and recently has become a rapid qualitative technique to examine electrodes modified with DNA molecules (e.g., gold electrodes covered with thiol-modified oligonucleotides^{19,23}). In our CV studies, we first performed voltammetry of AQS that had been intercalated into immobilized DNA molecules⁵⁴ in a TEA buffer. AQS, a polycyclic aromatic hydrocarbon (PAH), is known to be a DNA intercalator.^{12,15} Pandey and Weetall reported that one molecule of AQS can be bound to 51 nucleotide sites

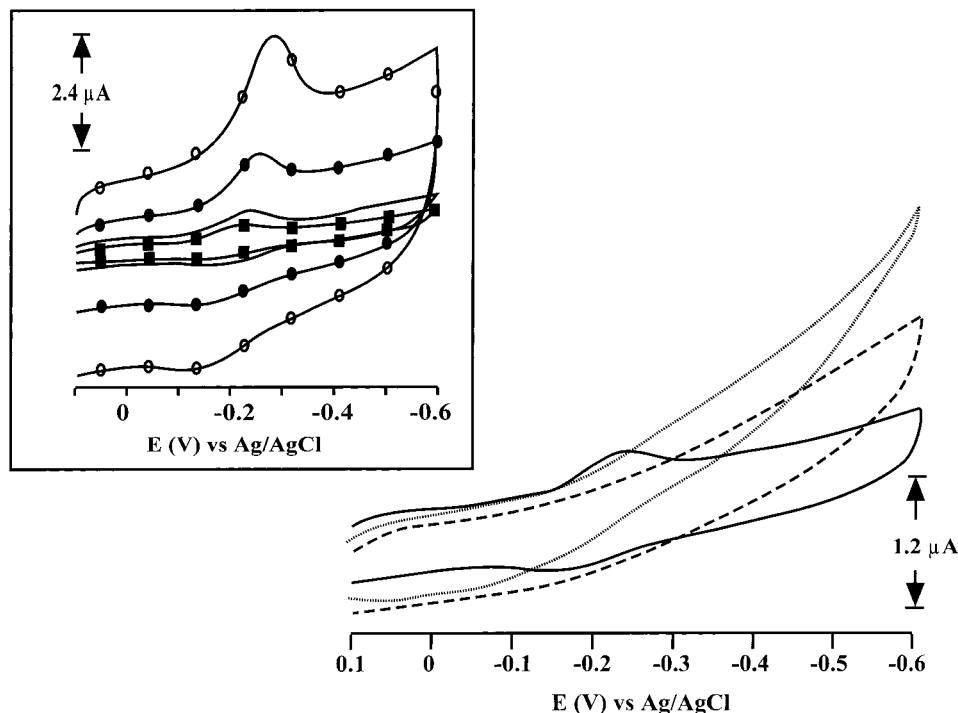


Figure 2. Cyclic voltammogram of 2,6-anthroquinonedisulfonic acid (AQS) that has been intercalated into immobilized calf thymus DNA (solid line curve) and two control voltammograms collected under same experimental conditions at an electrode modified only with MUA (dotted line curve) and at an electrode covered with a NHS ester-containing MUA film (dashed line curve), respectively. In all three experiments, the electrodes were immersed in 0.05 mM AQS solutions that were stirred overnight and then transferred into separate pH 8.0 TEA buffer solutions for the subsequent voltammetric experiments. The scan rate employed was 0.05 V/s. The inset shows the scan-rate dependence of the AQS reduction peak current. Scan rates used were 0.025 V/s (solid line curve with filled squares), 0.05 V/s (solid line curve), 0.2 V/s (solid line curve with filled circles), and 0.5 V/s (solid line curve with open circles).

of a DNA molecule.¹² They also characterized the voltammetric behaviors of AQS in the presence and absence of double-stranded DNA (ds-DNA) molecules.¹² Other PAHs or compounds containing PAH moieties, such as methylene blue²³ and tris(1,10-phenanthroline)cobalt(III) perchlorate,^{6,8,9,55} have also been used as indicators for the verification of successful DNA immobilization.

A typical voltammogram of AQS intercalated into DNA molecules immobilized using the aforementioned scheme and two control voltammograms are shown in Figure 2. These voltammograms were acquired in an attempt to address two possible complications, viz., the nonspecific binding of DNA onto MUA film and the adsorption of AQS onto surfaces that do not have DNA molecules. The comparison between the AQS voltammogram (solid line curve) and the control voltammogram obtained at a MUA-modified gold electrode that was also exposed to DNA solution (dotted line voltammogram) indicated that DNA would not be incorporated onto the MUA SAMs without the aid of NHS/EDC, confirming that there was no obvious nonspecific absorption of DNA molecules onto MUA SAMs. Considering that CV is a sensitive detection scheme for species present even in submonolayer quantity,¹⁷ the signal shown in the solid line curve must be associated with the AQS molecules that were intercalated into the surface-immobilized DNA molecules. The AQS reduction peak potential ($E_p \approx -0.25$ V) was found to be drastically different than -0.50 V, the peak potential of solution AQS measured from the voltammogram of a 50 μ M AQS/phosphate buffer solution at a bare gold electrode (voltammogram not shown, but in good agreement with voltammograms reported by Pandey and Weetall¹²). Such

a shift is indicative of the adsorbate nature of the intercalated AQS molecules. To further verify this, the scan-rate dependence of the cathodic peak, i_{pc} , was investigated over a wide range of scan rates, ν , and the resulting voltammograms are overlaid in the insert of Figure 2. Linear regression of normalized i_{pc} plotted against normalized ν (for a surface-confined species¹⁷) yielded $i_{pc} = 0.9199\nu + 0.00156$ with a R^2 value of 0.9999, while that of normalized i_{pc} plotted with respect to normalized $\nu^{1/2}$ (for a solution species¹⁷) produced $i_{pc} = 5.1098\nu^{1/2} - 5.3769$ with a R^2 value of 0.9714. The excellent fitting for the $i_{pc}-\nu$ plot vs the unsatisfactory fitting for the $i_{pc}-\nu^{1/2}$ and the slopes and intercepts again confirmed the adsorbate nature of AQS. We also studied the stability of the AQS-containing DNA film by repetitively cycling the electrode potential in the range depicted in Figure 2 and found no appreciable decrease of i_{pc} for 20–30 cycles. Thus, we conclude that most of the AQS detected were associated with the surface-confined DNA molecules, most likely through DNA intercalation.¹²

To clarify the second possible complication that may contribute to the interpretation of the AQS signal in Figure 2 (nonspecific adsorption of AQS onto NHS ester monolayers), voltammograms at electrodes covered with only MUA whose solution termini were modified with NHS esters were recorded. The absence of an AQS redox signal in the dashed voltammogram in Figure 2 again suggests that AQS molecules could not be accumulated onto electrode surfaces without surface-confined DNA.

The reason AQS has a low affinity toward the two types of films can be explained using the fact that there is electrostatic repulsion between the negatively charged AQS molecules and the anions present at these films. At neutral or basic pH, the solution ends of MUA were

(55) Wang, J.; Cai, X.; Rivas, G.; Vaiera, F. S.; Percio, A. M.; Shiraishi, H.; Palecek, E. *Electroanalysis* **1995**, *8*, 753–756.

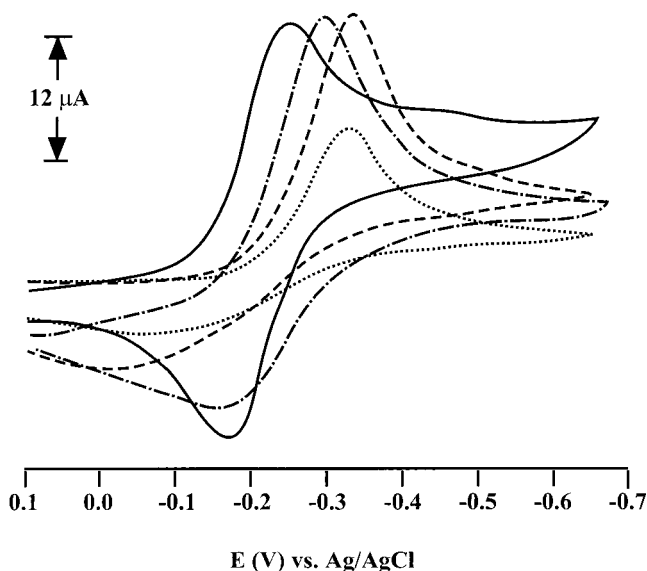


Figure 3. Cyclic voltammograms of 1.5 mM RuHex in pH 7.0 phosphate buffer obtained at a bare gold electrode (solid line curve), at a MUA-modified gold electrode (dashed line curve), at a gold electrode covered with NHS ester monolayers (broken dashed line curve), and at a gold electrode containing DNA (dotted line curve). The scan rate employed was 0.5 V/s.

reported to be deprotonated,³¹ while the sulfonate groups at the NHS ester monolayers rendered negative charges to the NHS ester monolayers. At both films, AQS molecules are repelled away from the electrode surfaces. We also attempted to immobilize DNA molecules in the presence of an excess amount of benzylamine and could not detect any trace amount of AQS that would be otherwise accumulated at the electrode surface. The results are described below in connection with the discussion of the physical implications of this work.

To qualitatively understand the surface organization and DNA coverage, a series of "blockage experiments" were conducted at MUA-, MUA/NHS-, and MUA/NHS/DNA-modified gold electrodes by recording the extent of reversibility and magnitudes of peak currents of solution RuHex at the respective electrode. The voltammetric behaviors of RuHex at these electrodes were then compared to response observed at a bare gold electrode. As can be seen in Figure 3, voltammograms of RuHex at film/monolayer-covered electrodes are less reversible than that acquired at a bare gold electrode. The shape of these voltammograms is similar to those of a reversible redox couple acquired at C₁₁-alkanethiol.⁵⁶ Moreover, peak currents of AQS at DNA-modified electrodes (see the dotted voltammogram in Figure 3), when compared to the voltammograms collected at electrodes that did not have DNA molecules, are greatly diminished. Such a phenomenon suggests that a large number of the pinholes or open areas present in the original MUA SAMs or NHS ester monolayers have been covered by DNA molecules. Similar data were obtained using poly[dG]·poly[dC], suggesting that our approach to immobilize DNA has been successful. To our knowledge, this is the first time that a voltammetric "blockage experiment" was performed at electrodes modified with biomolecules via the NHS/EDC cross-linking route.

Quartz Crystal Microbalance Results. In an attempt to quantify the amount of ds-DNA present at gold surfaces, we carried out quartz crystal microbalance (QCM) measurements of the frequency changes caused by the attached

Table 1. Concentration Dependence of Frequency Decrease, Amount of Immobilized Calf Thymus DNA, and the Number of Immobilized DNA Molecules per Unit Area

[DNA] ($\mu\text{g/mL}$) ^a	freq decrease (Hz) ^b	amt of immobilized DNA (ng)	immobilized DNA (molecules/cm ²) ^c
2	23	19.8	5.7×10^9
5	44	37.8	1.1×10^{10}
10	75	64.5	1.9×10^{10}
25	85	73.1	2.1×10^{10}
50	181	155.7	4.5×10^{10}
100	185	159.9	4.6×10^{10}

^a Three replicates were made for each concentration, and the average values are reported here. ^b Frequency decreases caused by the attachment of MUA SAMs and NHS esters were excluded. ^c The molecular weight of calf thymus was estimated to be 10.7×10^6 .

NHS and that associated with the subsequently immobilized DNA molecules. We decided to perform the frequency measurements using dried crystals because it has been recognized that QCM responses of solvated and tethered macromolecules might not be quantitatively related to mass changes due to the complicated situations in solution.⁵⁷ Table 1 summarizes the net frequency changes due to the attachments of calf thymus DNA molecules from solutions of different DNA concentrations. The total amount of DNA (in nanograms) across the entire gold disk on the QCM crystal at a given DNA concentration can be calculated according to the Sauerbrey equation^{38,58}

$$\Delta f = \frac{-2f_0^2}{A(\mu\rho)^{1/2}} \Delta m \quad (1)$$

where f_0 is the resonant frequency of the fundamental mode of the crystal, A is the area of the gold disk coated onto the crystal, ρ is the density of the crystal (2.648 g/cm^3), and μ is the shear modulus of quartz ($2.947 \times 10^{11} \text{ g/cm} \cdot \text{s}^2$). At a crystal of a 10 MHz fundamental frequency, a change of 1 Hz would correspond to 0.86 ng of materials adsorbed onto the surface of the crystal. By use of an estimated molecular weight of 10.7×10^6 for calf thymus DNA (containing 20 000 base pairs) and the area of the gold disk (0.196 cm^2), the number of DNA molecules per square centimeter can then be deduced. It should be pointed out that the frequency decrease listed in Table 1 has excluded the frequency change attributable to the NHS ester formation (typically within 20–25 Hz). In our treatment, we assume that the NHS esters replaced by DNA molecules would not cause a frequency decrease significant enough to introduce a large uncertainty. This assumption should be plausible based on the following argument and observation: (1) NHS is much lighter than the attached calf thymus DNA and therefore the detachment of NHS will result in a negligible frequency change when compared to the mass increase from the replacing DNA, and (2) the NHS ester hydrolysis rate during the time frame of the DNA immobilization is reported to be slow.^{27–29} Our AFM experiments, described below, also support such a finding. As a consequence, only a relatively small fraction of the total NHS esters present at the MUA SAMs will be replaced, introducing an uncertainty too small to change the interpretation of the results in Table 1. As will be seen below in connection with the comparison between AFM and QCM results, the biggest uncertainty

(57) Fawcett, N. C.; Craven, R. D.; Zhang, P.; Evans, J. A. *Anal. Chem.* **1998**, *70*, 2876–2880.

(58) Ward, M. D.; Buttry, D. A. *Science* **1990**, *249*, 1000–1007.

(56) Creager, S. E.; Rowe, G. K. *Langmuir* **1994**, *10*, 1186–1192.

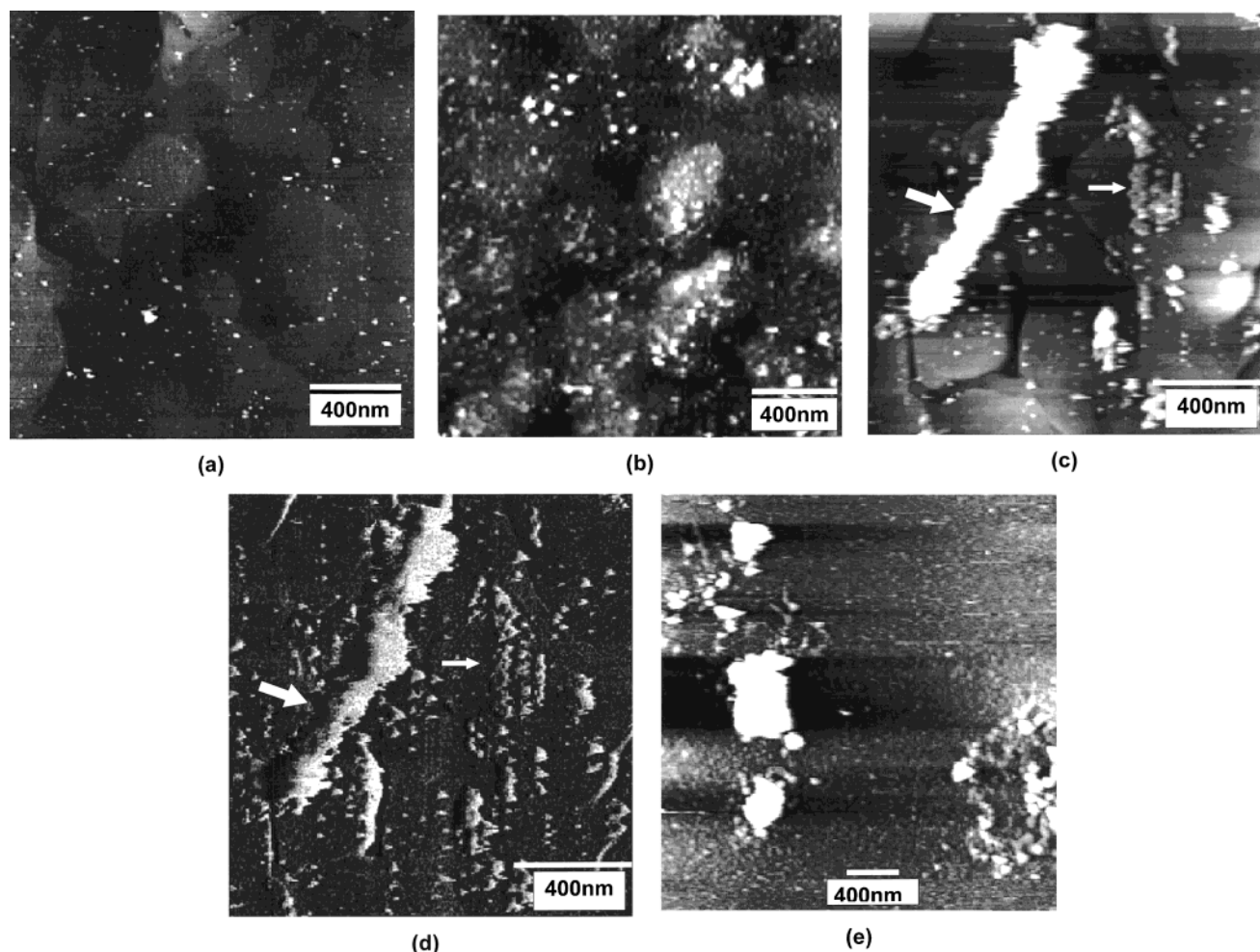


Figure 4. Topographical MAC mode AFM images of (a) a Au(111) substrate covered with a MUA film which had been exposed to a calf thymus DNA solution for 4 h, (b) a Au(111) substrate whose MUA adlayers were reacted with NHS/EDC for 4 h, and (c) calf thymus DNA molecules attached to a preformed MUA SAM via the NHS/EDC cross-linking scheme. Image (d) is the phase representation of the same area shown in image (c). Image (e) is a topographical AFM image of aggregates of calf thymus electrostatically adsorbed onto mica treated with (3-aminopropyl)triethoxysilane.

actually arises from our inability of taking DNA fragmentation into consideration.

Close examination of the values listed in Table 1 revealed that, when the DNA concentrations are around or less than 10 $\mu\text{g/mL}$, there is a somewhat linear relationship between the amount of immobilized DNA and the total DNA concentration in the solution. When the DNA concentration was higher than 10 $\mu\text{g/mL}$, the total number of immobilized calf thymus DNA molecules began to reach a constant value. The surface density of immobilized DNA is not even close to a full monolayer, as evidenced by the incomplete blockage of electron transfer of RuHex by DNA-modified electrode in Figure 3 and the AFM images shown below. Hence, the leveling off of the amount of immobilized DNA shown in Table 1 implies that once certain suitable sites containing activated carboxylic acids have been occupied by DNA molecules, further attachment of DNA molecules from the solution will become more difficult. Given the fact that the MUA-covered gold substrate was not fully covered by DNA molecules, it is not clear what hampered further attachment of DNA molecules. It is possible that the NHS ester groups are not well distributed or that a small fraction has undergone hydrolysis so that the organization of the activated carboxylic acid groups does not fit perfectly well with the spatial arrangements of the accessible DNA bases. Nevertheless, the leveling-off effect is consistent with our

CV measurements of AQS at electrodes that had been exposed to solutions of a wide range of DNA concentrations (5–100 $\mu\text{g/mL}$).

Atomic Force Microscope Experiments. To directly visualize the immobilized DNA and, more importantly, to determine the molecular orientation of DNA, MAC mode AFM was employed to examine gold substrates modified with calf thymus DNA. To correlate with our voltammetric characterization and QCM quantification of the surface-confined DNA, we also studied the MUA-covered gold substrate, MUA film exposed to DNA solution for 4 h, and a different MUA film that had undergone NHS/EDC reaction. Figure 4a shows the image of a gold substrate that was soaked in 1 mM MUA solution for 1 h, followed by exposure to a calf thymus DNA solution for 4 h. The displays of the individual islands of MUA molecules and the underlying grains of Au(111) are in good agreement with many STM and AFM images of gold surfaces covered with alkanethiol SAMs.^{42,44,46,47} The absence of DNA molecules at the MUA-covered gold substrate is consistent with our voltammetric experiment and confirms that there was no discernible nonspecific adsorption of DNA onto MUA film. The change brought by the exposure of MUA SAMs to the NHS/EDC solution for 4 h is shown in Figure 4b. The images became a little unclear with the disappearance of the previously resolvable MUA islands. This blurring of the image can presumably be ascribed to the

formation of a bulkier ester end group at the solution tail end of the MUA molecules. Despite the loss of the MUA islands, the gold grains can still be easily discerned. Our inability of detecting the individual MUA islands as shown in Figure 4a suggests that there was an extensive chemical modification of the MUA SAMs at the solution ends and the majority of the NHS esters did not undergo hydrolysis even after 4 h. The second point is in good agreement with observations made by Mattson et al.²⁹

In a separate experiment, a similar MUA film was fabricated, followed by DNA attachment in a mixture of NHS/EDC containing calf thymus DNA. A MAC mode AFM experiment was performed in an effort to identify the DNA molecules. Figure 4c is a topographical image of the resulting surface. As can be seen in this image, calf thymus DNA strands and fragments can be resolved (e.g., the strands indicated by the thin arrow in Figure 4c). Most of the small fragments on this image actually show the DNA helical structures. We also observed formation of small clusters of several long DNA strands (e.g., a typical cluster is indicated by the thick arrow in Figure 4c). The contrast of the phase image of DNA molecules over the same area (Figure 4d) is even more pronounced, owing to the enhancement arising from the sensitive detection of changes in the phase with the MAC mode detection.^{36,52} It is particularly evident from the comparison between the topographical representation of the small DNA cluster indicated by the thick arrow in Figure 4c and its phase counterpart shown in Figure 4d. To confirm that the strandlike motives are indeed associated with whole or fragments of calf thymus DNA molecules, we carried out a separate AFM imaging of calf thymus electrostatically adsorbed onto (3-aminopropyl)triethoxysilane (APTES)-treated mica surfaces. APTES is a common derivatization reagent to yield positive charges on mica surfaces for electrostatic adsorption of nucleic acids.⁴⁸ Because the distribution of APTES is not uniform and electrostatic adsorption cannot produce well-ordered DNA films, only DNA aggregates were observed. The width estimated from a resolvable strand among these intertwined DNA molecules on APTES-treated mica is about 22 ± 3 nm. This value compares well with the width of any typical DNA strand in Figure 4c (about 18 ± 3 nm). The apparent discrepancy between the above two values and the theoretical DNA strand width, 2 nm,⁵⁹ is mainly due to the image broadening affected by a combination of factors (e.g., the shape and size of the AFM tip, the sample preparation procedure, and AFM imaging in liquid environment) governing high-resolution AFM imaging.^{60,61} Comparing the strand widths from panels c and e of Figure 4, it is evident that the sample constructed through covalent binding and that prepared via electrostatic interaction resulted in slightly different AFM resolutions. Bustamante and co-workers reported that, under favorable conditions, widths of 12.6 ± 1.3 nm can be obtained from imaging nucleic acids in air with very sharp e-beam tips.⁶¹ Thudat et al. observed ds-DNA with average measured width to be 14 ± 2 nm even under careful humidity control.⁶² In fact, the widths we measured correlate well with those in many reported images of nucleic acids obtained at conventional AFM tips in liquid environment,

with values ranging from 15 to 25 nm.^{48,51,62-64} Therefore, we are confident that our AFM-detected DNA molecules tightly bound onto the preformed MUA SAMs.

Surface Coverage and Orientation of Immobilized DNA Molecules. An interesting point worth noting is that the observed DNA molecules appear to reside on top of the MUA films with the strands parallel to the underlying gold substrates (instead of extending into the solution as some of the rambling strands in the two DNA aggregates in Figure 4e are). This observation is based on the fact that depths of the DNA aggregates vary from 3 nm (e.g., that of the strands indicated by the thin arrow) to 5 nm (e.g., that of the clusters indicated by the thick arrow). These values are very close to the width of ds-DNA molecules,⁵⁹ again suggesting that the strandlike features arose from surface-confined DNA molecules and that the DNA strands were parallel to the electrode surface. Such arrangement suggests that the covalent bonding may have stretched the DNA strands upon immobilization, preventing individual DNA molecules from being interwoven into large aggregates. Even for small clusters of DNA (e.g., the one indicated by the thick arrow in Figure 4d), essentially all the DNA helices are lying flat on the substrate surface. Furthermore, the amide bond formation seems to lead to certain fragmentation of the native calf thymus DNA as some segments of DNA in Figure 3c are shorter than others. While we cannot completely rule out the possible shearing of calf thymus DNA due to other factors such as physical agitation, we believe that it is more likely that the relatively rigid MUA film and the fixed locations of the amide bonds produced the DNA strands of varying lengths.

We also attempted to estimate the surface density of DNA immobilized onto preformed MUA SAMs. Accurate determination of the number of DNA molecules from AFM images is limited by the uncertainty associated with resolving individual DNA molecules and by the relatively extensive DNA fragmentation. Moreover, the tiny area that the AFM probe examined (maximum scan area = $36 \mu\text{m}^2$) may not be representative of the entire gold surface (about $331\,000 \mu\text{m}^2$) in each imaging. Nevertheless, the surface density of DNA, averaged over four different areas of a surface such as that shown in Figure 4c, is 1.5×10^9 molecules/cm². Such a value is reasonable when compared to the surface density calculated from our QCM measurements of DNA molecules immobilized (e.g., 2.1×10^{10} molecules/cm² at $25 \mu\text{g/mL}$).

Physical Implications of the Characterization and Quantification of Surface-Confined DNA Molecules.

As stated in the Introduction, one of the objectives of the current work is to gain insight into the DNA immobilization process through the NHS/EDC cross-linking reaction. The pertinent issues include the organization of the DNA film (i.e., surface orientation and coverage), the nature of the DNA attachment (i.e., nonspecific adsorption vs covalent bonding), and the suitability of the scheme for the development of potential DNA sensors. While the first issue was addressed in the above section, it is worthwhile to present or reiterate the following observations/facts that deal with the other two issues.

While physical adsorption is a simpler way to attach biomolecules onto solid surfaces, the process is not trivial to control and the attached biomolecules might not be well ordered and tightly bound. We believe that, based on

(59) Lehninger, A. L.; Nelson, D. L.; Cox, M. M. *Principles of Biochemistry*; Worth Publishers: New York, 1993.

(60) Kossek, S.; Padste, C.; Tiefenauer, L. X. *Biosensors Bioelectron.* **1998**, *13*, 31-48.

(61) Bustamante, C.; Keller, D.; Yang, G. *Curr. Opin. Struct. Biol.* **1993**, *3*, 363-372.

(62) Thudat, T.; Allison, D. P.; Warmack, R. J.; Doktycz, M. J.; Jacobson, B. K.; Brown, G. M. *J. Vac. Sci. Technol.* **1993**, *11*, 824-828.

(63) Hansma, H. G.; Revenko, I.; Kim, K.; Laney, D. E. *Nucleic Acids Res.* **1996**, *24*, 713-720.

(64) Hansma, H. G.; Sinsheimer, R. L.; Groppe, J.; Bruce, T. C.; Elings, V.; Curley, G.; Beznilla, M.; Mastrangelo, I. A.; Hough, P. V. C.; Hansma, P. K. *Scanning* **1993**, *15*, 296-299.

the voltammetric and AFM studies of the MUA monolayers and NHS ester monolayers, the NHS/EDC cross-linking reaction should be the predominant, if not the sole, process for anchoring DNA molecules onto preformed MUA SAMs. Although surface IR spectroscopy may provide more direct evidence about the presence of the amide bonds, we feel that we have a sufficient amount of observations/arguments to bolster our contention. First, NHS esters must have been produced at the solution termini of the MUA SAMs since the aforementioned blurring of AFM images of the original MUA films indicated that the exposure to a NHS/EDC solution introduced certain changes to the surface. In a separate study, Frey and Corn reported Fourier transform IR (FTIR) spectroscopy measurements of the conversion of MUA to its NHS ester derivative³¹ under a condition similar to what we used. Second, calf thymus DNA molecules are huge polyanions, and therefore, without the formation of covalent bonds, would be strongly repelled by the sulfonate groups residing on the NHS esters. The phosphate buffer employed allows the DNA molecules to approach to the proximity of the NHS esters for the follow-up nucleophilic substitution, much in the same way as the buffer is used for bringing two single-stranded DNA molecules together to form a duplex.³ Our argument based on the electrostatic repulsion is analogous to that used for explaining the absence of nonspecific adsorption of AQS. The third fact is that, as mentioned in the preceding section, the DNA molecules seem to lie flat onto the preformed SAMs. Compared to the orientation and organization of DNA molecules anchored through electrostatic means, one would expect that, if DNA molecules were nonspecifically adsorbed, the resultant DNA orientation would be much more disordered.

To provide further evidence about the amide bond formation, we performed an NHS/EDC cross-linking reaction at a MUA-modified electrode immersed in a calf thymus DNA solution that also contained a large amount of benzylamine. Benzylamine is an aromatic primary amine that can competitively undergo the nucleophilic substitution reaction to replace the NHS esters. Because the concentration of benzylamine (4.58 mM) is much greater than that of DNA (4.67 nM) and benzylamine is significantly smaller and therefore more flexible to react with the MUA/NHS ester, the majority of the amide bonds will be that between the benzylamine and the carboxylic acid. Thus the number of immobilized DNA molecules will be greatly reduced. The small or negligible amount of DNA at the surface would not be able to accumulate a detectable amount of AQS. Indeed, when a large amount of benzylamine was used in the DNA immobilization step, the resulting voltammograms at electrodes that had been soaked into AQS solution were similar to the dotted voltammogram in Figure 2, suggesting that benzylamine attachment was prevalent. Wagner et al. and Mattson and co-workers cautioned that a small amount of amine compounds can drastically affect the efficiency of NHS/EDC cross-linking reaction for protein immobilization.^{29,33} Therefore, our benzylamine experiment is in line with their claim and consistent with the aforementioned facts/

arguments purporting the DNA attachment through the amide bond formation mechanism.

Since the NHS/EDC approach produces a better ordered DNA film with higher DNA surface density, covalent bonding should be the method of choice for developing heterogeneous DNA sensors with higher sensitivity and better hybridization efficiency. The ruggedness of DNA films formed with covalent bonding should also improve the reliability and reproducibility over DNA sensors constructed using electrostatic interactions. On the other hand, our AFM images suggest that some previously reported results from electrodes modified with polynucleotides through the NHS/EDC reaction should be reinterpreted by taking the DNA fragmentation associated with the amide bond formation into consideration.^{8,9} Therefore, we postulate that this method is probably a more suitable immobilization route to anchor smaller DNA molecules or single-stranded oligonucleotides since it is easier for such nucleic acids to fit the somewhat inflexible structure of the underlying alkanethiol SAMs. The relatively ordered arrangements of DNA strands and reasonable surface density suggest that NHS/EDC cross-linking should be, as many other researchers have discovered,^{31–33} a viable means to anchor certain biomolecules.

4. Conclusion

This work demonstrated that the integrated approach using voltammetry, QCM, and MAC mode AFM provides important insights to the nature of the DNA attachment, the surface coverage, orientation, and amount of DNA molecules that resulted from covalent attachment onto self-assembled alkanethiol monolayers. Our results indicate that the use of preformed MUA films for the subsequent NHS/EDC cross-linking of DNA produces DNA films that are better ordered than DNA molecules electrostatically adsorbed onto surfaces. Due to the relatively high surface coverage of DNA, we show, voltammetrically, that the surface-confined DNA molecules resulted in a significant blockage of the sites in SAMs that were originally available for facile electron transfer of an electroactive species. We also found that an electroactive DNA intercalator can be incorporated into and tightly bound to the surface-confined DNA molecules. We demonstrate that MAC mode AFM is capable of examining the suitability of the NHS/EDC scheme for the immobilization of DNA molecules. Our results indicate that, while DNA molecules can be attached and films of DNA with a reasonably high surface coverage can be fabricated, the formation of amide bonds tends to fragment large polynucleotides. Thus, the method will be more appropriate to the immobilization of oligonucleotides or certain protein molecules.

Acknowledgment. Support for this work by the National Institutes of Health—Minority Biomedical Research Support is gratefully acknowledged. F.Z. also acknowledges The donors of the Petroleum Research Fund, administered by the American Chemical Society.

LA9910834